



Article

Comparative Genomic Analysis of a Novel *Vibrio* sp. Isolated from an Ulcer Disease Event in Atlantic Salmon (*Salmo salar*)

Maryam Ghasemieshkaftaki ¹, Ignacio Vasquez ¹, Aria Eshraghi ² , Anthony Kurt Gamperl ³ and Javier Santander ^{1,*}

¹ Marine Microbial Pathogenesis and Vaccinology Laboratory, Department of Ocean Sciences, Memorial University of Newfoundland, St. John's, NL A1C 5S7, Canada; mghasemieshk@mun.ca (M.G.); ivasquezsol@mun.ca (I.V.)

² Department of Infectious Diseases & Immunology, University of Florida, Gainesville, FL 32608, USA; ariaeshraghi@ufl.edu

³ Fish Physiology Laboratory, Department of Ocean Sciences, Memorial University of Newfoundland, St. John's, NL A1C 5S7, Canada; kgamperl@mun.ca

* Correspondence: jsantander@mun.ca; Tel.: +1-709-864-3268

Abstract: Ulcer diseases are a recalcitrant issue at Atlantic salmon (*Salmo salar*) aquaculture cage-sites across the North Atlantic region. Classical ulcerative outbreaks (also called winter ulcer disease) refer to a skin infection caused by *Moritella viscosa*. However, several bacterial species are frequently isolated from ulcer disease events, and it is unclear if other undescribed pathogens are implicated in ulcer disease in Atlantic salmon. Although different polyvalent vaccines are used against *M. viscosa*, ulcerative outbreaks are continuously reported in Atlantic salmon in Canada. This study analyzed the phenotypical and genomic characteristics of *Vibrio* sp. J383 isolated from internal organs of vaccinated farmed Atlantic salmon displaying clinical signs of ulcer disease. Infection assays conducted on vaccinated farmed Atlantic salmon and revealed that *Vibrio* sp. J383 causes a low level of mortalities when administered intracelomic at doses ranging from 10^7 – 10^8 CFU/dose. *Vibrio* sp. J383 persisted in the blood of infected fish for at least 8 weeks at 10 and 12 °C. Clinical signs of this disease were greatest 12 °C, but no mortality and bacteremia were observed at 16 °C. The *Vibrio* sp. J383 genome (5,902,734 bp) has two chromosomes of 3,633,265 bp and 2,068,312 bp, respectively, and one large plasmid of 201,166 bp. Phylogenetic and comparative analyses indicated that *Vibrio* sp. J383 is related to *V. splendidus*, with 93% identity. Furthermore, the phenotypic analysis showed that there were significant differences between *Vibrio* sp. J383 and other *Vibrio* spp., suggesting J383 is a novel *Vibrio* species adapted to cold temperatures.

Keywords: Atlantic salmon; *Vibrio* sp. J383; genomics; phylogenetics; phenotype; ulcer disease



Citation: Ghasemieshkaftaki, M.; Vasquez, I.; Eshraghi, A.; Gamperl, A.K.; Santander, J. Comparative Genomic Analysis of a Novel *Vibrio* sp. Isolated from an Ulcer Disease Event in Atlantic Salmon (*Salmo salar*). *Microorganisms* **2023**, *11*, 1736. <https://doi.org/10.3390/microorganisms11071736>

Academic Editor: Eman Zahran

Received: 3 June 2023

Revised: 21 June 2023

Accepted: 27 June 2023

Published: 2 July 2023



Copyright: © 2023 by the authors. Licensee MDPI, Basel, Switzerland. This article is an open access article distributed under the terms and conditions of the Creative Commons Attribution (CC BY) license (<https://creativecommons.org/licenses/by/4.0/>).

1. Introduction

Ulcerative diseases in Atlantic salmon (*Salmo salar*) aquaculture were first reported in Norway in 1980, and still are a significant health/economic issue for the North Atlantic region [1]. The Gram-negative marine pathogen *Moritella viscosa* is typically described as the etiological agent of the classic ulcer disease (also called winter ulcer disease) in European farmed fish [2,3]. Although *M. viscosa* is the primary pathogen associated with ulcer disease, it is not the only bacterium isolated from ulcers and lesions in Atlantic salmon. The isolation and identification of various bacterial species from ulcer-disease cases have been reported, including *Alivibrio wodanis* (formerly *Vibrio wodanis*) and *Tenacibaculum* sp. [4,5]. In fact, *Tenacibaculum* might target scarified skin, and co-infect wounds with *M. viscosa* [5]. Also, *M. viscosa* might co-infect with *A. wodanis*, which may limit the growth of *M. viscosa* [6]. In addition, *A. wodanis* has the ability to solo infect Atlantic salmon [7].

Since the first documented outbreak of ulcerative disease in Eastern Canada (summer 1999) caused by *A. wodanis* in Atlantic salmon [8], several pathogens including *M.*

viscosa and *Tenacibaculum* spp. have been isolated [5,9]. Despite broad immunization with polyvalent vaccines containing *M. viscosa* antigens, ulcerative-disease events continue to be reported, causing poor fillet quality and financial losses [10,11]. This suggests that undescribed bacterial species may be involved in ulcer disease pathology [11], and that they are not covered by current vaccines.

The occurrence of ulcerative disease in Norway and other European countries is significantly different from in Canada. In European countries, ulcerative disease occurs below 7 °C [12]. However, in Canada, ulcerative disease frequently occurs in summer and mid-autumn when water temperatures are over 10 °C [13]. The mortality rate caused by ulcerative disease is less than 10% in Norwegian farms during winter outbreaks, and fish that survive recover when the water temperature increases above 8 °C in spring [9]. In Atlantic Canada, the highest cumulative cage-level mortality recorded was 31.2% in the first described outbreak [8]; however, it seems that mortality has decreased over time, although its frequency has increased [13].

Skin-ulcer disease in Atlantic salmon is relatively unexplored, and there is limited published data on this disease in Atlantic salmon on the east coast of Canada [13,14]. Salmon farmers report that skin ulcers in sea-cages can progress very fast. At first, fish may only have laterally raised scales, and after a few days, they die with a single large circular ulcerative lesion of several centimeters in diameter [14]. Actually, in Atlantic Canada, “summer” skin ulcers in Atlantic salmon lead to significant mortality rates and economic losses [13].

In this study, we isolated a novel *Vibrio* sp. J383 strain from vaccinated farmed Atlantic salmon exhibiting clinical signs of skin ulcer disease, and characterized its phenotype and genome. Infection assays revealed that *Vibrio* sp. J383 does not cause an acute infection, but instead causes a chronic infection in Atlantic salmon. Comparative genomics analyses suggest that *Vibrio* sp. J383 is a new species that might contribute to skin ulcer disease in Atlantic salmon.

2. Materials and Methods

2.1. Phenotypic Characterization

2.1.1. Isolation

Farmed Atlantic salmon vaccinated with ALPHA JECT exhibiting clinical signs of ulcer disease at 12 °C (Figure 1) were netted and immediately euthanized with an overdose of MS-222 (400 mg/L; Syndel Laboratories, BC, Canada). Tissue samples (spleen, head kidney, and liver) were collected and placed into sterile homogenizer bags (Nasco whirl-pak®, Fort Atkinson, WI, USA, then weighed and homogenized in phosphate-buffered saline [PBS; 136 mM NaCl, 2.7 mM KCl, 10.1 mM Na₂HPO₄, 1.5 mM KH₂PO₄ (pH 7.2) up to a final volume of 1 mL] [15]. From the homogenized tissue suspension, 100 µL was plated onto Trypticase Soy Agar (TSA; Difco, Franklin Lakes, NJ, USA) supplemented with up to 2% NaCl and incubated at 15 °C for 48–72 h. Colonies were streak purified on agar for further analysis [16]. Bacterial stocks were preserved at –80 °C in 10% glycerol and 1% peptone solution. A single colony of each isolated bacteria was grown in 3 mL Trypticase Soy Broth (TSB) supplemented with 2% NaCl in a 16 mm diameter glass tube and placed in a drum roller (TC7, New Brunswick Scientific, MA, USA) for 24 h at 15 °C with aeration (180 rpm). When required, TSB was supplemented with 1.5% bacto-agar (Difco) and 0.02% Congo-red (Sigma-Aldrich, Burlington, MA, USA) [17,18]. Luria Bertani (LB; yeast extract 5 g; tryptone 10 g; NaCl 10 g; dextrose 1 g) with different concentrations of NaCl (0, 0.5, 2%) was used to evaluate halophilic growth [19].



Figure 1. *Vibrio* sp. J383 strain was isolated from the spleen of Atlantic salmon exhibiting clinical signs of skin ulcers.

2.1.2. Biochemical, Enzymatic and Physiological Characterization

The biochemical profile of *Vibrio* sp. J383 was characterized using API 20E, API 20NE, and API ZYM according to the manufacturer's (BioMerieux, Marcy-l'Etoile, France) instructions. The strips were incubated at 15 °C for 48 h, and the results were analyzed using API web (BioMerieux). The primary characterization of *Vibrio* sp. J383 was performed based on the Gram stain, capsule stain, and morphological and cultural characteristics [16]. *Vibrio* sp. J383 growth rate was determined in TSB with 2% NaCl at 4, 15, 28, and 37 °C. Halophilic growth was evaluated in LB supplemented with 0.5 and 2% of NaCl. Also, catalase and oxidase activity were measured according to standard protocols [16,19]. Hemolytic activity was assessed in TSA with 5% salmon blood and sheep blood agar at 15 °C [19,20]. The bacteria's liposaccharide (LPS) profile was examined based on previous protocols [21,22]. *Vibrio* sp. J383 growth curves were determined in triplicate at 15 °C according to established protocols [18].

2.1.3. Antibiogram

The susceptibility to antimicrobials was determined using sensi-disc diffusion tests [23]. Briefly, *Vibrio* sp. J383 susceptibility was determined for tetracycline (10 µg), oxytetracycline (30 µg), ampicillin (10 µg), sulfamethoxazole (STX) (25 µg), chloramphenicol (30 µg), colistin sulphate (10 µg), and oxalic acid (2 µg) using standard methods [19,23].

2.1.4. Siderophore Synthesis

A siderophores secretion assay was performed using CAS plates according to standard procedure [24]. Briefly, previously mentioned conditions were used to cultivate *Vibrio* sp. J383, and mid-log phase bacteria with an optical density (O.D.) at 600 nm of 0.7 were harvested, washed three times with PBS at 6000 rpm for 10 min, and then resuspended in 1 mL of PBS. This bacterial culture was used to inoculate TSB with 2% NaCl, and TSB with 2% NaCl supplemented with 100 µM of FeCl₃ or 100 µM of 2,2 dipyridyl in a ratio 1:10 (bacteria: culture media). *Vibrio* sp. J383 was cultured under aeration for 24 h at 15 °C. The cells were collected at the mid-log phase after the incubation time, washed twice with PBS, and resuspended in 100 µL of PBS. After that, CAS agar plates were inoculated with 5 µL of the concentrated bacterial pellet and incubated at 15 °C for 48 h [24].

2.2. Infection Trials

2.2.1. Fish Origin and Holding Conditions

Farmed Atlantic salmon (~200–250 g) of New Brunswick (Saint John River) origin that had been vaccinated with ALPHA JECT micro IV (Pharmaq, Overhalla, Norway) were held at the Joe Brown Aquatic Research Building (Ocean Sciences Center, Memorial

University; MUN) in 3800 L tanks supplied with 95–100% air saturated, and UV-treated, flow through seawater at 10–12 °C, and an ambient photoperiod (spring–summer). The fish were fed three days per week at 1% body weight with a commercial dry pellet (Skretting, BC, Canada; 50% protein, 18% fat, 1.5% carbohydrate, 3% calcium, 1.4% phosphorus). All experiments were conducted under approved institutional animal ethics protocols (#18-1-JS and #18-03-JS).

2.2.2. Bacterial Inoculum Preparation

Isolated strains were grown, harvested, and used to infect the Atlantic salmon. Briefly, bacterial cells were harvested at the mid-log phase, at an O.D. at 600 nm of ~0.7, and washed three times with PBS at 6000 rpm for 10 min. Bacterial O.D. was monitored using a Genesys 10 UV spectrophotometer (Thermo Spectronic, Thermo Fischer Scientific, MA, USA) and by plating to determine the colony forming units (CFU/mL) [25,26].

2.2.3. Koch's Postulates

The infection procedures were conducted in the AQ2 biocontainment unit at the Cold-Ocean Deep-Sea Research Facility (CDRF), MUN. Fish were transferred to the AQ2-CDRF unit and acclimated for one week at 10 °C before infection. An initial infection screening assay was conducted in Atlantic salmon (200 g) intraperitoneally (ip) injected with a high dose (1×10^8 CFU/dose) of each isolated strain. Each infected group consisted of 5 fish in individual tanks under optimal conditions. Fish ip injected with PBS were used as a negative control, and fish ip injected with *M. viscosa* J311 (ATCC BAA-105) were used as a positive control.

A total of 135 Atlantic salmon (~250 g) were used to evaluate Koch's postulates for *Vibrio* sp. J383 [15,26,27]. The infection procedures were conducted according to established protocols [25,28]. Briefly, fish were anesthetized with 0.05 g/L MS-222 and individually injected with 100 µL of the respective bacterial inoculum. Fish were divided into three 500 L tanks containing 45 Atlantic salmon each, and intracelomic (ic) infected with 10^6 , 10^7 , and 10^8 CFU/dose, respectively. Mortality was monitored until 12 weeks post-infection (wpi). The water temperature was increased during the experiment, starting at 10 °C for 4 wpi, then raised to 12 °C at 5 wpi, and finally increased to 16 °C at 9 wpi until 12 wpi. Tissue samples (e.g., head kidney, liver, spleen, and blood) from 6 fish of each dose were aseptically taken at 2 wpi. Bacterial loads were determined by established protocols [25,28]. Briefly, liver, spleen and head kidney were aseptically removed, and sections of the collected tissues were placed into sterile homogenizer bags (Nasco whirl-pak®, Fort Atkinson, WI, USA), weighed, and PBS was added to a final volume of 1 mL. Then, the tissues were homogenized, the suspensions were serially diluted (1:10), and then plated onto TSA supplemented with 2% NaCl. To determine the number of bacteria CFU per g of tissue, the plates were incubated at 15 °C for at least 5 days. The total bacterial count was normalized to 1 g of tissue according to the initial weight of the tissue as previously described [25]. Additionally, blood samples were taken from 6 fish per dose every two weeks until the end of the experiment (i.e., at 2, 4, 6, 8, 10, and 12 wpi). Heparin (100 mg/mL) was added to the blood samples, serially diluted in filtered sterilized seawater (1:10) and plated in TSA with 2% NaCl.

Since mortality was evident at 12 °C, a second infection trial was conducted only at 12 °C. A total of 160 Atlantic salmon (~250 g) were equally distributed in four 500 L tanks containing 40 fish each and acclimated at 12 °C for one week before infection. One group of fish was not infected and used as a negative control. Fish in the other group were ic injected with 10^8 CFU/dose of *Vibrio* sp. J383. Blood samples were collected randomly from 9 fish every two weeks to determine the bacterial load until 14 wpi. Also, tissue samples (e.g., head kidney, liver, and spleen) were collected at 12 and 14 wpi from 9 fish. This experiment was conducted according to established protocols [25,28], and mortality was monitored daily until 12 wpi.

2.3. *Vibrio* sp. J383 Genomics

2.3.1. *Vibrio* sp. J383 DNA Extraction and Sequencing

Vibrio sp. J383 was grown, harvested, and washed as previously described. According to the manufacturer's instructions (Promega, Madison, WI, USA), the Wizard Genomic DNA Purification Kit was used to extract the genomic DNA (gDNA) of *Vibrio* sp. J383. The gDNA was quantified by spectrophotometer using a Genova Nano Micro-Spectrophotometer (Jenway, UK) and evaluated for purity and integrity by electrophoresis (0.8% agarose gel) [29]. Libraries and sequencing were conducted at Genome Quebec (Canada) using PacBio and Miseq Illumina sequencers.

2.3.2. Genome Assembly, Annotation and Data Submission

Celera Assembler (August 2013 version) was used to assemble the PacBio readings. The assembled contigs were analyzed using a CLC genomic workbench (Qiagen, v22.0). Genome annotations were conducted using the Rapid Annotation Subsystem Technology pipeline (RAST 2.0.) (<http://rast.nmpdr.org/>; accessed on 2 February 2023) [30,31], and PATRIC (<https://www.patricbrc.org>; accessed on 2 February 2023) [32]. The *Vibrio* sp. J383 genome was submitted to the National Center for Biotechnology Information (NCBI) for public accessibility and re-annotated using the NCBI Prokaryotic Genome Annotation Pipeline. The *Vibrio* sp. J383 chromosomes and plasmid genomes were visually mapped using CG view software (<https://cgview.ca/>) (accessed on 20 June 2023).

2.3.3. Comparative Genomics Analysis

Average nucleotide identity (ANI) was calculated by whole genome alignments using the CLC genomic workbench whole genome analysis tool with default parameters.

(Min. initial seed length = 15; Allow mismatches = yes; Min. alignment block = 100). A minimum similarity of 0.8 and a minimum length of 0.8 were used as parameters for CDS identity. A comparative heat map was made using CLC. Phylogenetic analysis was performed using two different software packages, CLC Genomic workbench v22.0 and MEGA11 [33]. Evolutionary history was estimated using the Neighbor-Joining method with a bootstrap consensus of 500 replicates [34], and evolutionary distance was computed using the Jukes–Cantor method [35]. *Photobacterium damselae* 91-197 (AP018045/6) chromosomes were utilized as an outgroup [36]. Whole genome dot plots between closely related strains were constructed using the whole genome analysis tool to visualize and analyze genomic differences. Comparative alignment analysis was conducted using the CLC genomic workbench (Qiagen, v22.0). This analysis was used to identify homologous regions (locally collinear blocks), translocations, and inversions within the two bacterial genomes for chromosomes 1 and 2.

2.3.4. Genomic Islands

The detection of genomic islands (GIs) was conducted using the Island Viewer v.4 pipeline (<https://www.pathogenomics.sfu.ca/islandviewer/browse/>; accessed on 1 February 2023), which integrates Island Path-DIMOB, SIGH-HMM, and Island Pick analysis tools into a single platform [37]. Analysis was performed for both chromosomes and the plasmid. SecReT6 v3 web server was utilized to identify and annotate the type VI secretion system (T6SS) genes that share sequence homology with characterized T6SSs [38,39].

2.4. Statistical Analysis

Fish survival rates were transformed using an arc-sin (survival rate ratio) function. One-way ANOVAs were utilized to identify significant differences. GraphPad Prism 9 was used to conduct all statistical analyses (GraphPad Software, California, CA, USA).

3. Results

3.1. Phenotypic Characterization

Vibrio sp. J383 displayed substantial growth in TSB with 2% NaCl between 15 °C and 4 °C (Table 1). However, it did not grow well at 28 °C and did not grow at 37 °C. *Vibrio* sp. J383 grew well in LB with 1% and 2% NaCl at 15 °C. However, it did not grow in LB supplemented with 0 and 0.5% NaCl at 15 °C. These results indicated that *Vibrio* sp. J383 is psychotropic and halophilic. *Vibrio* sp. J383 showed hemolytic activity in sheep and salmon blood agar at 15 °C (Figure S1G,I). *Vibrio* sp. J383 was shown to be motile, oxidase and catalase-positive, and type I-fimbria-negative (Table 1).

Table 1. Phenotypic characteristics of *Vibrio* sp. J383.

Characteristics (Growth at)	<i>Vibrio</i> J383
Gram Stain	Gram-Negative
Capsule stain	+
Hemolysin in Salmon blood agar(15 °C)	+
Hemolysin in Sheep blood agar (15 °C)	+
Hemolysin in Salmon blood agar(28 °C)	—
Hemolysin in Sheep blood agar (28 °C)	—
Type 1 fimbria	—
Growing in LB 0% NaCl (15 °C)	—
Growing in LB 0.5% NaCl (15 °C)	—
Growing in TSB 2% NaCl (4 °C)	+
Growing in TSB 2% NaCl (15 °C)	+
Growing in TSB 2% NaCl (28 °C)	+
Growing in TSB 2% NaCl (37 °C)	—
Motility Test	+
Catalase	+
Oxidase	+
Biofilm	+
Antibiogram using sensi-disk of:	Halo diameter (mm)
Vibriostatic agent (O-129)	25 (Susceptible)
Tetracycline (10 µg)	30 (Susceptible)
Oxytetracycline (30 µg)	30 (Susceptible)
Ampicillin (10 µg)	23 (Susceptible)
Sulfamethoxazole (25 µg)	25 (Susceptible)
Chloramphenicol (30 µg)	30 (Susceptible)
Colistin sulphate (10 µg)	0 (Resistant)
Oxalic acid (2 µg)	24 (Susceptible)

To evaluate siderophore synthesis, *Vibrio* sp. J383 was grown under iron-enriched and iron-limited conditions, inoculated onto CAS agar plates, and incubated at 15 °C for 48 h. Siderophore secretion was observed under iron-enriched (100 µM of FeCl₃), iron-limited (100 µM of 2,2 dipyridyl), and control conditions (TSB). Furthermore, there were no noticeable differences in the size of the halo for siderophore secretion between different groups (Figure S1B).

Vibrio sp. J383 produces a capsule and a smooth lipopolysaccharide (LPS) profile (Figure S1C,D).

The biochemical and enzymatic profiles indicated that *Vibrio* sp. J383 can synthesize alkaline phosphatase, esterase (C4), esterase lipase (C8), lipase (C14), leucine, valine, and cysteine arylamidase, acid phosphatase, naphthol-AS-BI phosphohydrolase, and galactosidase (Table S1). *Vibrio* sp. J383 reduces nitrates and glucose, produces indole from tryptophan, produces esculinase and gelatinase, β-galactosidase and can utilize D-mannitol, D-glucose and D-amygdaline (Table S1). The API 20NE profile 7474004 indicated that the isolate could be *V. vulnificus* or *V. alginolyticus* with 64.8% and 34.6% confidence, respectively (Table S1).

3.2. Antibiogram

The antibiogram analysis showed that *Vibrio* sp. J383 is colistin-sulphate-resistant, but susceptible to ampicillin, tetracycline, oxytetracycline, sulfamethoxazole, chloramphenicol, oxalic acid, and the vibriostatic agent O-129 (Table 1). These results are similar to other *Vibrio* spp. strains [40].

3.3. Infection Trials in Atlantic Salmon

We isolated a total of five strains, three from the head kidney, one from the liver, and one from the spleen, from different infected fish. An initial screening to determine the virulence of the five isolates was conducted in Atlantic salmon (200 g). The fish were transferred to the AQ2/3 biocontainment zone of the CDRF, acclimated for 1 week, and intraperitoneally (ip) injected with a very high dose (1×10^8 CFU/dose) of each isolate. Fish ip injected with PBS were used as a negative control, and fish ip injected with *M. viscosa* J311 were used as a positive control. As expected, *M. viscosa* killed all the animals quickly, and all the animals ip injected with PBS survived (Figure S2). Only the strain J383 (SP6) caused mortality and clinical signs of ulcer disease. Mortality associated with J383 infection in Atlantic salmon indicates that it causes a chronic type of infection rather than an acute infection. This is consistent with the infection event from which these samples were obtained.

The first infection trial was conducted to evaluate Koch's postulates under rising temperature conditions (10 °C for 4 weeks, 12 °C for 4 weeks, and 16 °C for 4 weeks). Approximately 22.5% mortality was recorded in the high-dose (10^8 CFU/dose) group, 5% mortality rate in the medium-dose (10^7 CFU/dose) group, and no mortality was observed in the low-dose (10^6 CFU/dose) group (Figure 2A). Mortality started at 10 °C, peaked at 12 °C, but was not reported at 16 °C. Clinical signs and presence of *Vibrio* sp. J383 were observed in all moribund Atlantic salmon (Figure 2B). *Vibrio* sp. J383 was not detected in internal organs and blood samples at 2 wpi, but it was detected in blood in the high-dose infection group at 4, 6, 8 and 10 wpi. *Vibrio* sp. J383 was detected in the blood of fish infected with the medium dose at 6 and 10 wpi. However, at 12 wpi, no bacteria were observed in the collected samples from the different doses (Table 2). The isolation of *Vibrio* sp. J383 from blood samples confirmed Koch's postulates.

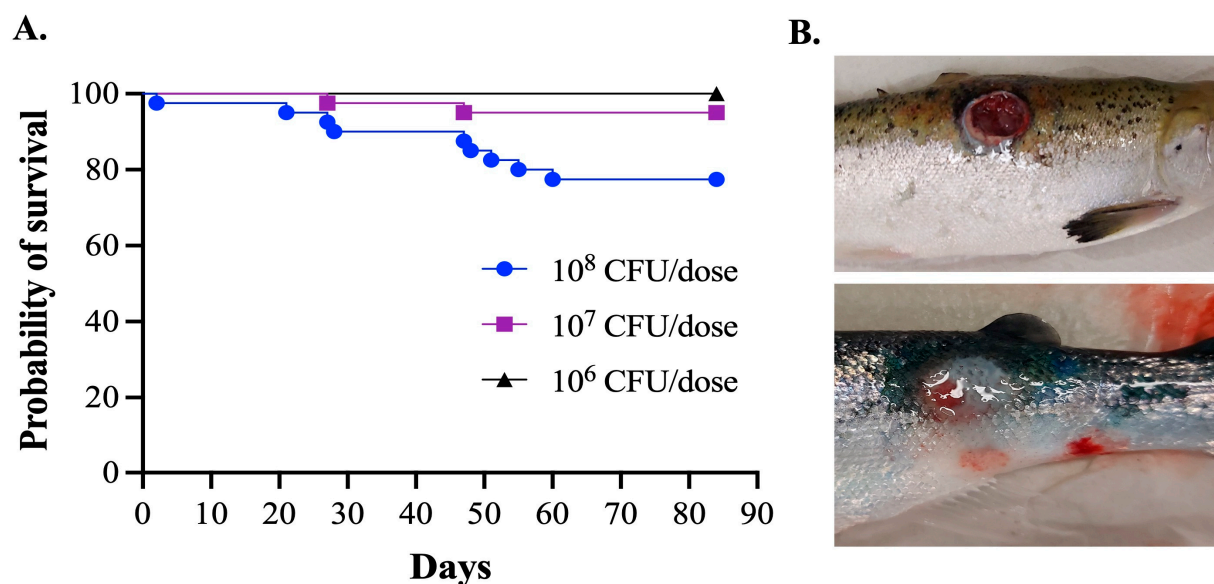


Figure 2. Survival and clinical signs of Atlantic salmon interperitoneally infected with *Vibrio* sp.: (A) Mortality of Atlantic salmon infected with *Vibrio* sp. J383; and (B) clinical sign of Atlantic salmon infected with *Vibrio* sp. J383.

Table 2. *Vibrio* sp. J383 isolated from blood samples at different time points post-infection (weeks post-infection: wpi).

Positive Samples for <i>Vibrio</i> spp. J383 (Total Positive/6 Fish)						
Temperature	10 °C		12 °C		16 °C	
	Dose	2 wpi	4 wpi	6 wpi	8 wpi	10 wpi
10 ⁶		0/6	0/6	0/6	0/6	0/6
10 ⁷		0/6	0/6	1/6	0/6	1/6
10 ⁸		0/6	3/6	4/6	3/6	2/6

A second infection assay was performed at 12 °C to determine the infection kinetics of *Vibrio* sp. J383, with 10⁸ CFU/dose. Mortality started at 5 dpi and reached 20% by 90 dpi (Figure 3). *Vibrio* sp. J383 caused bacteremia in about 30–100% of the infected fish, and reached a peak at 6 wpi, which is consistent with the mortality levels (Figures 3 and 4A). Bacteremia started to decrease by 8–10 wpi. No bacteria in the blood were detected after 12 wpi (Figure 4A), but *Vibrio* sp. J383 was detected in the spleen, liver, and head kidney at this sampling point (Figure 4B). Higher bacterial loads were observed in the spleen samples compared to the liver and head kidney (Figure 4B).

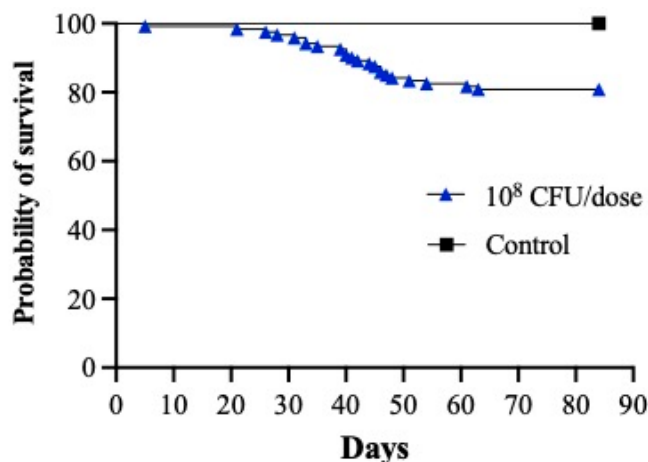


Figure 3. Survival portion of Atlantic salmon interperitoneally infected with *Vibrio* sp. J383 at a high dose at 12 °C.

3.4. *Vibrio* sp. J383 Genomics

Vibrio sp. J383 gDNA sequenced by PacBio and MiSeq revealed the presence of two chromosomes and one large plasmid. *Vibrio* sp. J383 chromosome 1 (NZ_CP097293.1) has 3,633,265 bp, chromosome 2 (NZ_CP097294.1) 2,068,312 bp, and the large plasmid pJ383 (NZ_CP097295.1) 201,166 bp (Figure 5A–C). The coverage assembly for chromosome 1, chromosome 2, and the parge plasmid was 306, 27, and 14 times, respectively. The plasmid profile agrees with the genomic analysis, supporting the theory that this *Vibrio* sp. possesses one large plasmid and no small plasmids. *Vibrio* sp. J383's genome was submitted to NCBI under the BioProject (PRJNA836625) and BioSample (SAMN28165975). *Vibrio* sp. J383 genome has a total estimated length of 5.9 Mb and a G + C content of 44.3 and 44.1% for chromosomes 1 and 2, respectively. RAST pipeline annotation predicted a total of 309 subsystems and 3235 coding sequences (CDS) for chromosome 1, a total of 101 subsystems and 1866 CDSs for chromosome 2, and a total of 8 subsystems and 237 CDSs for the large plasmid pJ383 (Table 3). The NCBI Prokaryote Genome Annotation pipeline (PGAP) presented a total of 5288 genes predicted, a total of 16 (5S), 15 (16S), and 15 (23S) rRNAs, 138 tRNAs, and 5 ncRNAs for the whole genome (Table 4).

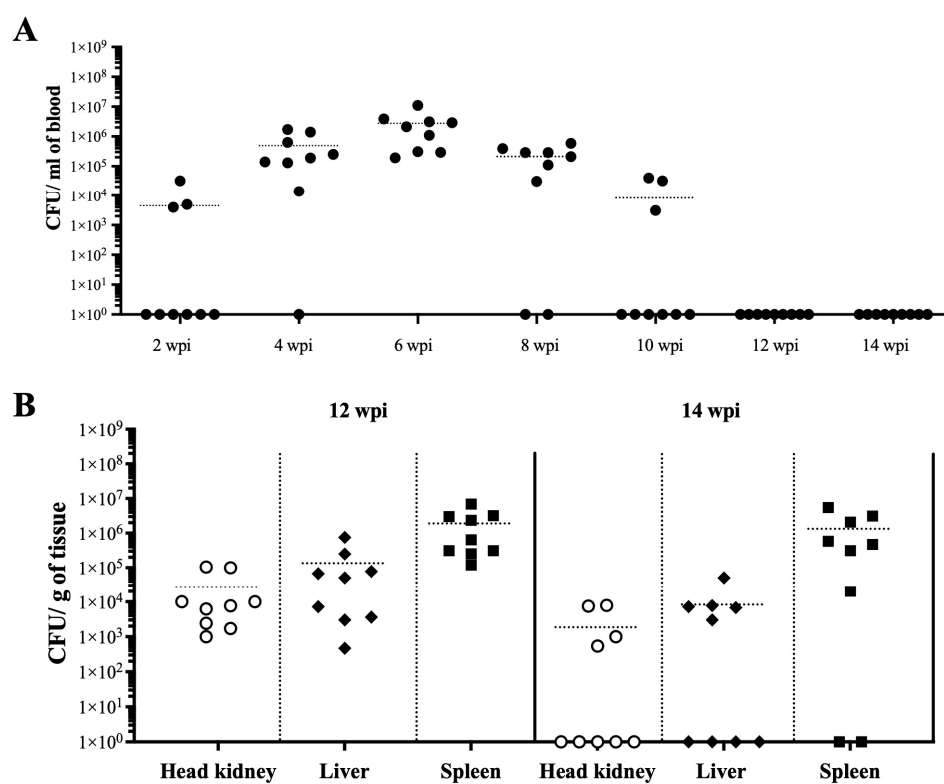


Figure 4. *Vibrio* sp. J383 blood and tissue colonization in vaccinated farmed Atlantic salmon. (A) *Vibrio* sp. J383 loads in blood of ($n = 9$) infected fish with the high dose (1×10^8 CFU/dose) at 2, 4, 6, 8, 10, 12 and 14 wpi; and (B) *Vibrio* sp. J383 loads in head kidney, liver, spleen of ($n = 9$) infected fish with the high dose (1×10^8 CFU/dose) of *Vibrio* sp. J383 at 12 and 14 wpi. Full circle: blood; empty circle: head kidney; full roboid: liver; full square: spleen.

Table 3. Rapid annotation subsystem technology (RAST) *Vibrio* sp. J383 annotation.

Characteristics	Chromosome-1	Chromosome-2	Plasmid
Genome size (bp)	3,633,265	2,068,312	201,166
G + C content (%)	44.3	44.1	43.4
Number of subsystems	309	101	8
Number of coding sequences	3235	1866	237
Number of RNAs	163	21	0

Table 4. Prokaryotic genome annotation summary (*Vibrio* sp. J383).

Attribute	Data Provider
Annotation Pipeline	NCBI prokaryotic Genome Annotation pipeline
Annotation Method	Best-placed reference protein set; GeneMarkS-2+
Genes (total)	5288
CDSs (total)	5099
Genes (coding)	5031
CDSs (with protein)	5031
Genes (RNA)	189
rRNAs	16, 15, 15 (5S, 16S, 23S)
Complete rRNAs	16, 15, 15 (5S, 16S, 23S)
tRNAs	138
ncRNAs	5
Pseudo Genes (total)	68
CDSs (without protein)	68
Pseudo Genes (ambiguous residues)	0 of 68
Pseudo Genes (frameshifted)	29 of 68
Pseudo Genes (incomplete)	33 of 68
Pseudo Genes (internal stop)	21 of 68
Pseudo Genes (multiple problems)	13 of 68

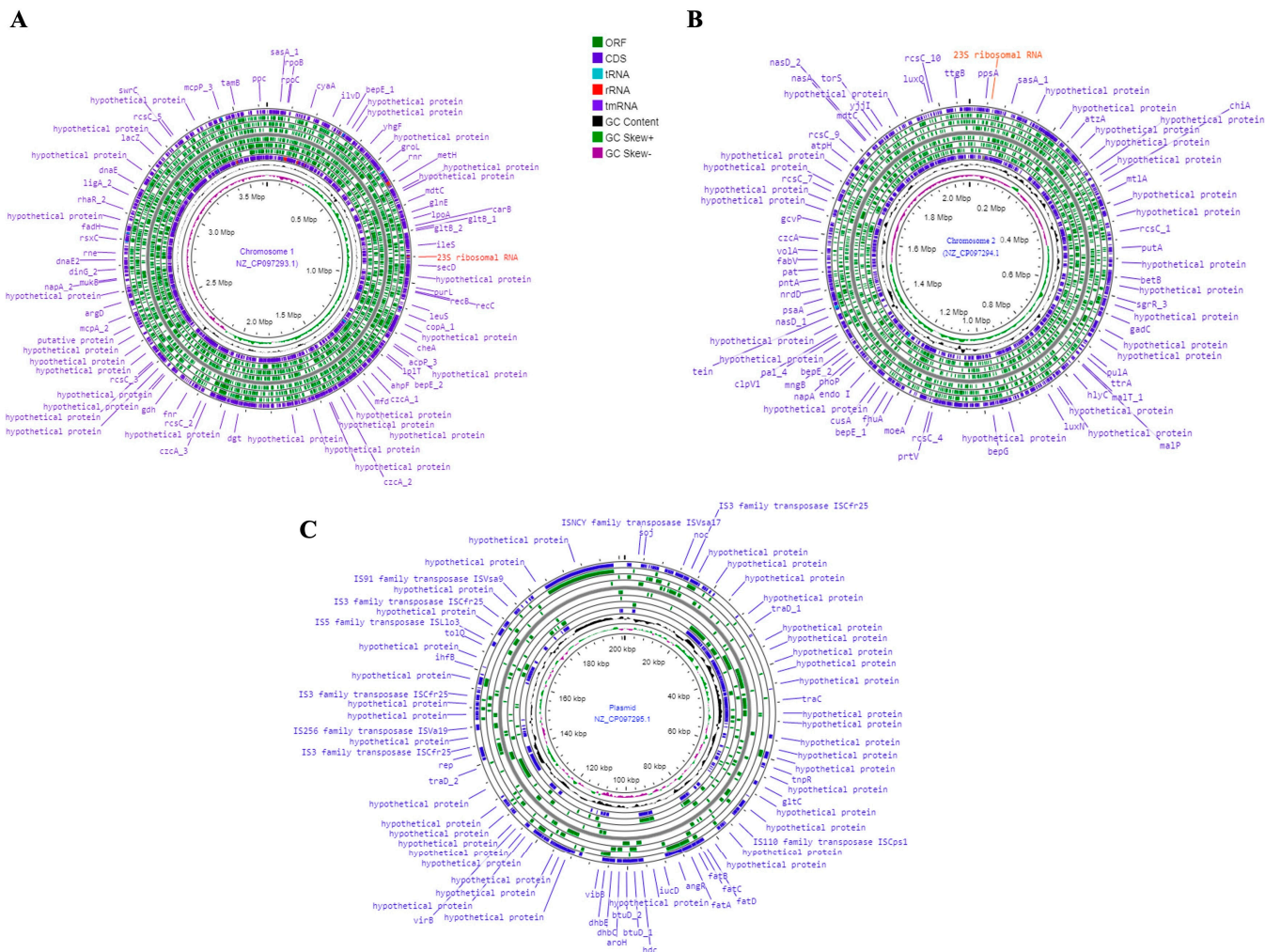


Figure 5. *Vibrio*. sp. J383 chromosomes. (A) *Vibrio*. sp. J383 chromosome 1 genome visualization; (B) *Vibrio*. sp. J383 chromosome 2 genome visualization; and (C) genome map representation of the large plasmid of *Vibrio* sp. J383. A circular graphical display of the distribution of the genome annotations is provided. This includes, from outer to inner rings, the contigs, CDS on the forward strand, CDS on the reverse strand, RNA genes, CDS with homology to known antimicrobial resistance genes, CDS with homology to known virulence factors, GC content and GC skew.

3.5. Genomic Islands (GIS)

Twenty-four putative GIs were identified within the chromosomes and plasmid: sixteen GIs in chromosome 1, seven GIs in chromosome 2, and one GI in the plasmid (Figure 6A–C). The GIs' size ranged from 6 kb to 50 kb, with a total of 929 genes (Supplementary Files S1–S3). Genes encoding for integrases, transposases, phage integrase, and multidrug-resistance transporters were found in GIs 6, 7, 9 and 12, respectively. Also, UDP-3-O-[3-hydroxymyristoyl] glucosamine N-acyltransferase, virulence factor VirK and alpha-galactosidase were in GIs 3, 7 and 15, respectively. Zonula occludes toxin (Zot)-like phage protein was found in the chromosome 1 of *Vibrio* sp. J383. Glutaredoxin encoding gene was detected in genomic island 20 of chromosome 2.

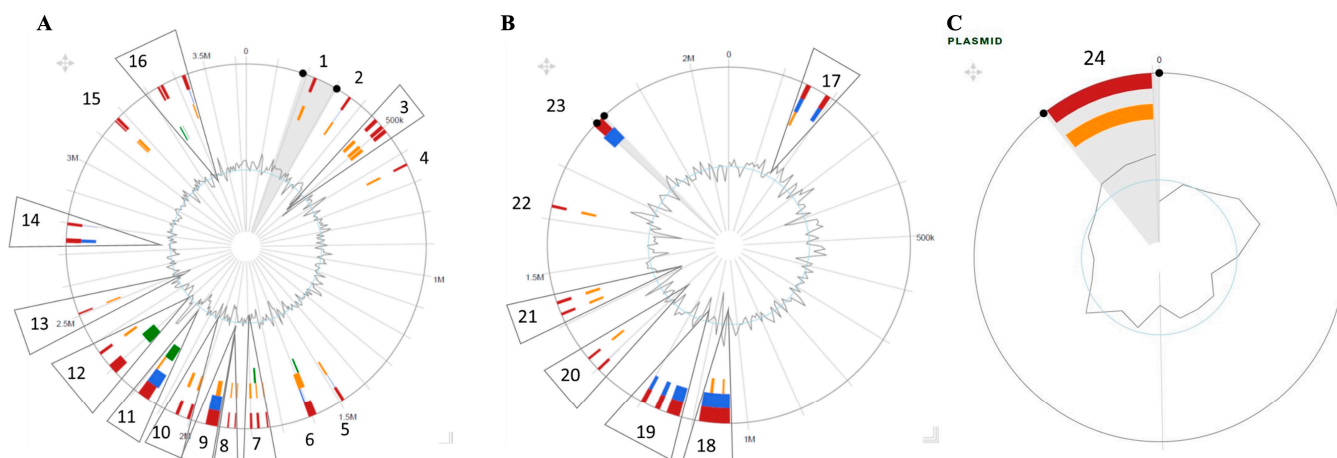


Figure 6. Genomic islands (GIs) detected in *Vibrio* sp. J383. (A) Chromosome 1 and (B) chromosome 2; and (C) genomic islands (GIs) detected in plasmid. Red bars represent GIs detected using 3 different packages; blue bars represent the GIs detected with SIGI-HMM package; orange bars represent the GIs detected with the Island Path-DIMOB package; green bars represent the GIs detected with the Island Pick package.

The type VI secretion system (T6SS) is an important virulence factor detected in *Vibrio* sp. J383. The SecReT6 v3 web server identified and annotated the T6SS genes that share sequence homology with characterized T6SSs and indicated that the *Vibrio* sp. J383 genome encodes two distinct T6SSs in GI 12 of chromosome 1 and GI 21 of chromosome 2 (Table 5, Figure 7, and Supplementary Files S4 and S5). The *Vibrio* sp. J383 secretion systems belong to the T6SSⁱ family and are most closely related to the T6SS in *Vibrio corallilyticus* OCN008. Some genes encoded within these two loci do not share sequence homology with known T6SS genes; however, predicting the structures of the encoded proteins with AlphaFold and comparison to solved structures in the Protein Data Bank (<http://rcsb.org>) (last accessed on 20 June 2023) allowed us to identify additional T6SS genes [41]. These analyses indicate that both T6SS loci in the *Vibrio* sp. J383's genome encode for the full complement of components required for T6SS assembly and activity [42].

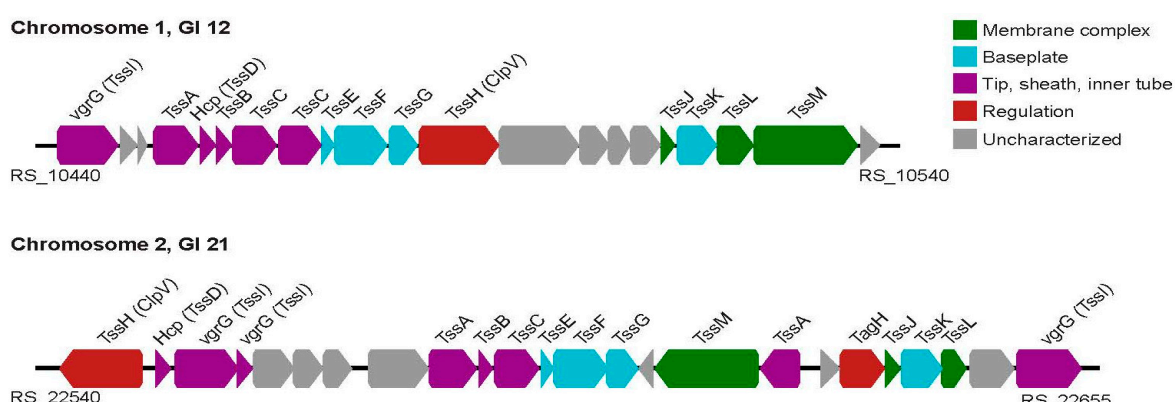


Figure 7. Type VI secretion system (T6SS) gene cluster in *Vibrio* sp. J383. The T6SS in chromosomes 1 and 2 are made from 13 Tss (Type Six Subunits) proteins that are known as the “core components”. TssC gene duplicated in chromosome 1. Several uncharacterized genes are present in two T6SS loci and these may encode toxins secreted by the apparatus; however, further characterization is required to elucidate the role of these genes.

Table 5. Genes of type VI secretion system (T6SS) in *Vibrio* sp. J383.

Gene	Locus Tag	Chromosome/GI	Location(nt)	Putative Function
<i>vgrG</i>	M4S28_RS10440	1/12	2,282,509	Tip of the T6SS apparatus
	M4S28_RS10445	1/12	2,284,552	Unknown
	M4S28_RS10450	1/12	2,285,122	Unknown
<i>tssA</i>	M4S28_RS10455	1/12	2,285,641	Cap of the T6SS sheath
<i>hcp</i>	M4S28_RS10460	1/12	2,287,140	Inner tube of the T6SS
<i>tssB</i>	M4S28_RS10465	1/12	2,287,681	T6SS sheath
<i>tssC</i>	M4S28_RS10470	1/12	2,288,184	T6SS sheath
<i>tssC</i>	M4S28_RS10475	1/12	2,289,701	T6SS sheath
<i>tssE</i>	M4S28_RS10480	1/12	2,291,095	T6SS baseplate
<i>tssF</i>	M4S28_RS10485	1/12	2,291,510	T6SS baseplate
<i>tssG</i>	M4S28_RS10490	1/12	2,293,326	T6SS baseplate
<i>tssH</i>	M4S28_RS10495	1/12	2,294,306	Disassembly of the T6SS apparatus
	M4S28_RS10500	1/12	2,296,928	MFS transporter
	M4S28_RS10505	1/12	2,299,492	ABC transporter protein
	M4S28_RS10510	1/12	2,300,477	Transporter protein
	M4S28_RS10515	1/12	2,301,209	FHA domain-containing protein
<i>tssJ</i>	M4S28_RS10520	1/12	2,302,156	T6SS membrane complex
<i>tssK</i>	M4S28_RS10525	1/12	2,302,686	T6SS baseplate
<i>tssL</i>	M4S28_RS10530	1/12	2,304,023	T6SS membrane complex
<i>tssM</i>	M4S28_RS10535	1/12	2,305,222	T6SS membrane complex
	M4S28_RS10540	1/12	2,308,694	AarF/UbiB family protein
<i>tssH</i>	M4S28_RS22540	2/21	1,384,843	Disassembly of the T6SS apparatus
<i>hcp</i>	M4S28_RS22545	2/21	1,387,991	Inner tube of the T6SS
<i>vgrG</i>	M4S28_RS22550	2/21	1,388,584	Tip of the T6SS apparatus
<i>vgrG</i>	M4S28_RS22555	2/21	1,390,662	Tip of the T6SS apparatus
	M4S28_RS22560	2/21	1,391,173	Unknown
	M4S28_RS22565	2/21	1,392,473	Unknown
	M4S28_RS22570	2/21	1,393,458	Unknown
	M4S28_RS22575	2/21	1,394,912	Unknown
<i>tssA</i>	M4S28_RS22580	2/21	1,396,905	Cap of the T6SS sheath
<i>tssB</i>	M4S28_RS22585	2/21	1,398,497	T6SS sheath
<i>tssC</i>	M4S28_RS22590	2/21	1,399,012	T6SS sheath
<i>tssE</i>	M4S28_RS22595	2/21	1,400,548	T6SS baseplate
<i>tssF</i>	M4S28_RS22600	2/21	1,400,969	T6SS baseplate
<i>tssG</i>	M4S28_RS22605	2/21	1,402,714	T6SS baseplate
	M4S28_RS22610	2/21	1,403,742	Lrp/AsnC transcriptional regulator
<i>tssM</i>	M4S28_RS22615	2/21	1,404,255	T6SS membrane complex
<i>tssA</i>	M4S28_RS22620	2/21	1,407,701	Cap of the T6SS sheath
	M4S28_RS22625	2/21	1,409,679	Unknown
<i>tagH</i>	M4S28_RS22630	2/21	1,410,294	Regulatory
<i>tssJ</i>	M4S28_RS22635	2/21	1,411,783	T6SS membrane complex
<i>tssK</i>	M4S28_RS22640	2/21	1,412,295	T6SS baseplate
<i>tssL</i>	M4S28_RS22645	2/21	1,413,617	T6SS membrane complex
	M4S28_RS22650	2/21	1,414,557	Unknown
<i>vgrG</i>	M4S28_RS22655	2/21	1,416,026	Tip of the T6SS apparatus

3.6. Comparative Genomic Analysis

The phylogenetic analysis of *Vibrio* sp. J383 chromosomes indicated that it was closely related to *V. splendidus* (Figure 8A–D). The average nucleotide identity (ANI) analysis between *Vibrio* sp. J383 and *V. splendidus* showed 95.75% identity for chromosome 1 (Figure S3A) and 93.31% identity for chromosome 2 (Figure S3B), which suggests that these two strains share a common ancestor.

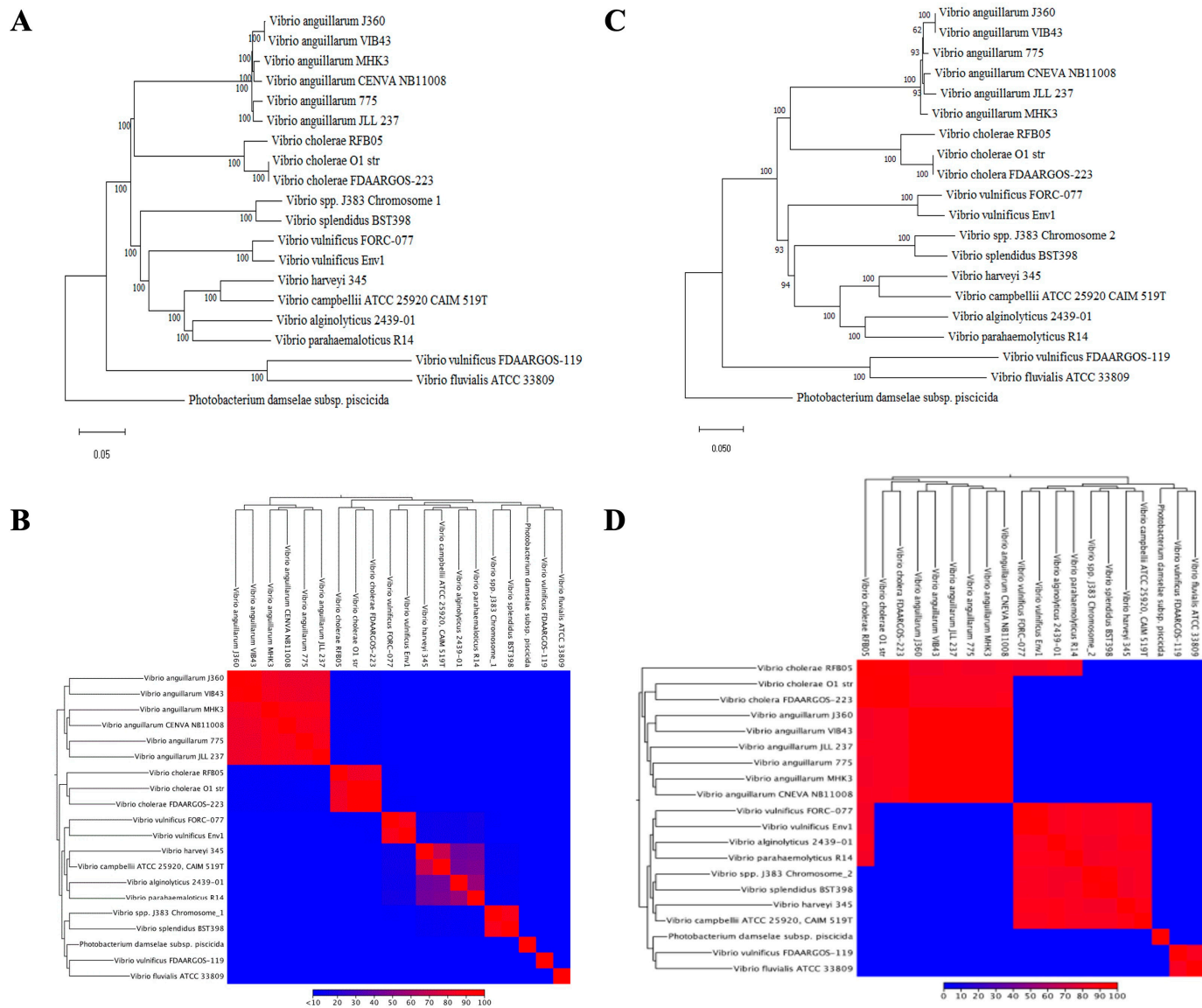


Figure 8. Phylogenetic history of *Vibrio* sp. J383 genome. (A) Chromosome 1 evolutionary history was inferred using the neighbor-joining method, with a bootstrap consensus of 500 replicates for taxa analysis in MEGA 11 software; (B) heat map visualization of aligned sequence's identities for *Vibrio* sp. J383 chromosome 1; genome alignment involved 20 *Vibrio* sp. analysis in CLC; and (C) chromosome 2 evolutionary history was inferred using the neighbor-joining method, with a bootstrap consensus of 500 replicates for taxa analysis in MEGA 11 software. (D) Heat map visualization of aligned sequences identified for *Vibrio* sp. J383 chromosome 2 genome alignment. This involved 20 *Vibrio* sp. and analysis in CLC.

However, the dot plot showed significant differences between *Vibrio* sp. J383 and *V. splendidus* in both chromosomes (Figure 9A,C), including genome gaps and one inversion event in chromosome 1 (Figure 9A,B).

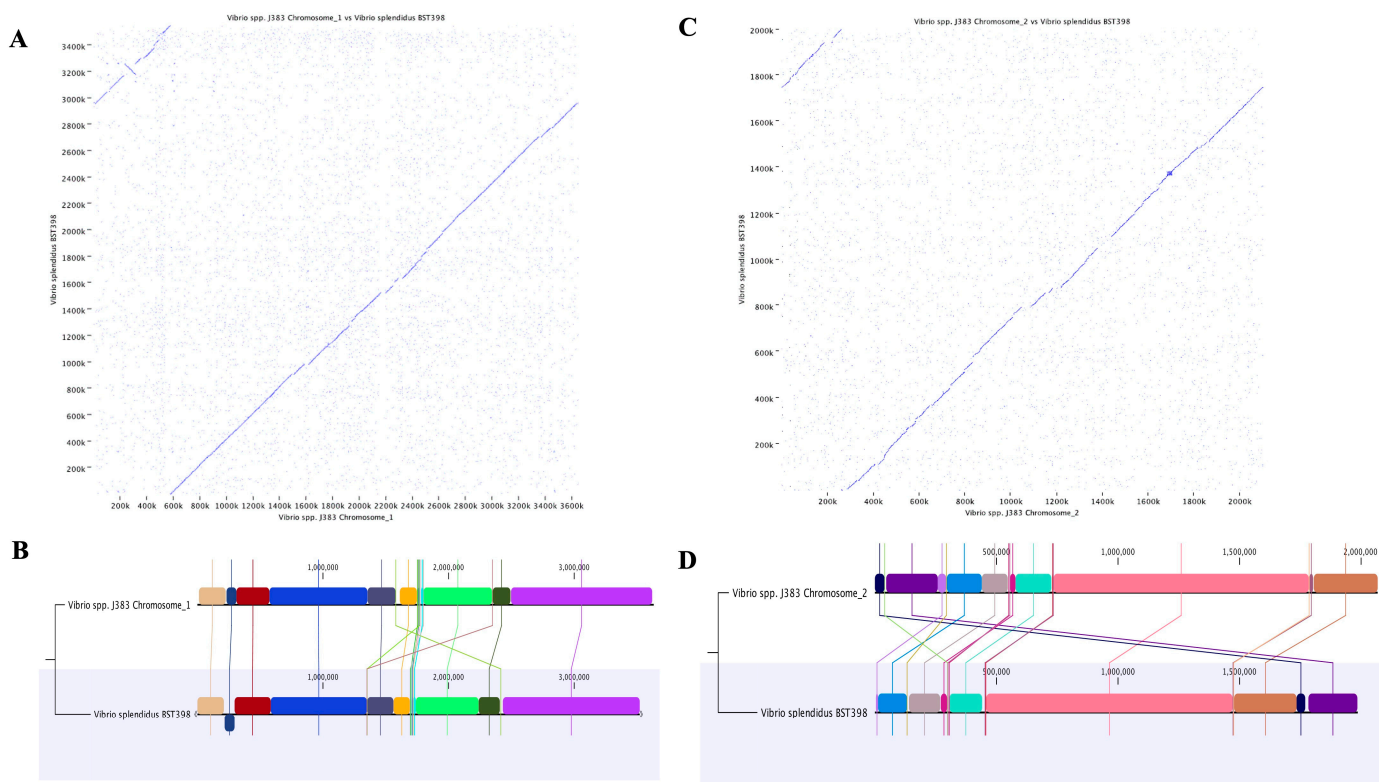


Figure 9. Comparative genome synteny between *Vibrio* sp. J383 and *V. splendidus* BST 398. **(A)** Dot plot analysis for chromosome 1; dot plots were computed using CLC Genomics Workbench v.20; blue arrow represents inversion. **(B)** Homologous regions identified as locally colinear blocks (LCBs) of chromosome 1. **(C)** Dot plot analysis for chromosome 2; Dot plots were computed using CLC Genomics Workbench v.20. **(D)** Homologous regions identified as locally colinear blocks of chromosome 2.

The whole genome alignment identified 18 locally collinear blocks (LCBs) in *Vibrio* sp. J383, which are conserved segments with no genomic rearrangements [43]. The comparative alignment analysis of each chromosome showed 9 LCBs in chromosome 1 (Figure 9B) and 9 LCBs in chromosome 2 (Figure 9D).

Also, comprehensive genome analysis in PATRIC indicated that there were some pathogenesis-associated genes. Chromosomes 1 and 2 contain several transporter-related genes as well as genes linked to virulence or antibiotic resistance. RAST and PATRIC comprehensive genome analyses identified the presence or absence of specific genes in the chromosomes and the plasmid (Table S2).

4. Discussion

The causes of ulcerative skin disease in Atlantic salmon are not fully understood. Several causative agents are being described in the North Atlantic rim, including *M. viscosa*, *Tenebrioebacillus* spp., and *A. wondanidis* [4,5]. However, differences in disease etiology indicate that several undescribed pathogens might also cause skin ulcers in Atlantic salmon. In the present study, we isolated *Vibrio* sp. strain J383 from the spleen of Atlantic salmon exhibiting skin ulcers (Figure 1). The phenotypic characterization indicates that this strain is marine and requires the presence of at least 1% of NaCl for survival (Table 1 and Figure S1A). Also, *Vibrio* sp. J383 showed substantial growth between 4 and 15 °C, but no growth at temperatures over 28 °C, suggesting that this strain is adapted to cold temperatures. *Vibrio* sp. J383 also possesses several virulence factors, including hemolysins, siderophores, and LPS (Table 1, Figure S1B,D,G,I), indicating that it has pathogenic properties. Finally, *Vibrio* sp. J383 constitutively synthesizes siderophores, indicating that this strain can scavenge essential iron within and outside the host. The synthesis of siderophores is

usually regulated [44], but *Vibrio* sp. J383 possesses a natural constitutive expression that requires further study.

Infection assays indicated that *Vibrio* sp. J383 is a non-acute, chronic pathogen that can produce skin ulcers and kill fish, especially at 12 °C (Figures 2 and 3). *Vibrio* sp. J383 triggered clinical signs of ulcer disease in vaccinated farmed Atlantic salmon, indicating that the generic vaccine utilized does not confer protection against this novel chronic pathogen (Figure 2B). Skin ulcer severity ranged from mild to severe in some of the fish that were infected with medium and high doses (10^7 and 10^8 CFU/dose, respectively) (Figure 2B). Although clinical signs of ulcer disease were evident in the infected fish, the low mortality rates indicated that this strain is not an acute pathogen. Around 5% to 22.5% mortality was recorded in the infected fish given the medium and high doses of *Vibrio* sp. J383 (Figure 2A). Our result is consistent with the literature, which indicates that the mortality during outbreaks in sea-cages with skin ulcers ranged from 0.01 to 23.32% [13]. *Vibrio* sp. J383 caused bacteremia, and it was detected until 10 wpi in Atlantic salmon at 12 °C. Bacteremia showed the same patterns in both infection assays (Figure 4A, Table 2). This indicates that *Vibrio* sp. J383 can cause a systemic infection. *Vibrio* sp. J383 was detected at 6 wpi in most of the blood samples in the high-dose infection group (Table 2), and isolated in all the blood samples at 12 °C (Figure 4A). Bacteremia was not recorded at 10 °C at 2 wpi but was reported at 12 °C in some blood samples (Table 2, Figure 4A). No bacteremia and mortality were recorded when the temperature increased to 16 °C (Table 2). These results are consistent with previous field observations, which indicated that the water temperature during skin ulcerative disease outbreaks ranged from 10 °C to 13 °C [13]. Our findings indicated that *Vibrio* sp. J383 becomes more invasive at 12 °C compared to 10 °C. Regardless of water temperature, *Vibrio* sp. J383 was not detected in the blood at 12 wpi (Table 2, Figure 4A). However, *Vibrio* sp. J383 was detected in the spleen, head kidney, and liver at 12 and 14 wpi in Atlantic salmon infected with the high dose at 12 °C (Figure 4B). Bacterial loads were significantly higher in the spleen compared to the liver and head kidney at 12 and 14 wpi. *Vibrio* sp. J383 loads decreased substantially from 12 wpi to 14 wpi (Figure 4B). Collectively, our findings suggest that *Vibrio* sp. J383 is a chronic pathogen.

The biochemical characterization and identification of environmental *Vibrio* species have been complicated because of their notable diversity [45,46]. The biochemical profile attained using API 20NE showed that *Vibrio* sp. J383 was unable to reduce urea but reduces nitrates and produces indole, suggesting 64.8% and 34.6% similarity to *V. vulnificus* and *V. alginolyticus*, respectively (Table S1). Phylogenetic and comparative analyses showed that *Vibrio* sp. J383 is closely related to *V. splendidus*, with 93% identity, and this suggests that these two strains share a common ancestor. However, phenotypical tests revealed significant differences between *Vibrio* sp. J383 and other *Vibrio* strains, indicating that *Vibrio* sp. J383 could be a novel species.

V. anguillarum J360, a virulent strain isolated from the North Atlantic, displayed thermo-inducible α -hemolysin activity at 28 °C, but no hemolytic activity at 15 °C [15]. In contrast, *Vibrio* sp. J383 showed hemolysin activity at 15 °C but not at 28 °C. *Vibrio* spp. utilize hemolysins to lyse host erythrocytes to acquire nutrients, such as iron [47]. Hemolysins are crucial virulence factors for *V. anguillarum* and play a key role in boosting its pathogenicity [48,49]. The presence of hemolytic activity in *Vibrio* sp. J383 indicates its potential pathogenicity. *Vibrio* sp. J383 showed growth at 4 °C, optimal growth around 15 °C, weak growth at 28 °C and no growth at 37 °C. Also, *Vibrio* sp. J383 produces catalase and oxidase. These results are consistent with most pathogenic marine *Vibrio* spp. [50], and the ability of *Vibrio* sp. J383 to grow at 4 °C indicates that this novel pathogen is well adapted to cold environments.

The genotypic characterization of *Vibrio* sp. J383 indicated the presence of two chromosomes. The existence of two chromosomes is a basic characteristic of *Vibrio* spp. that developed as a survival means, and allows for the rapid adaptation of the pathogen to different environments and hosts [51]. *Vibrio* sp. J383 has a genome size of 5,902,734 bp, very similar to *V. splendidus* BST 398, (5,508,387 bp) (Table 3). The genome of *V. splendidus*

BST 398 included 4700 predicted open reading frames, a G + C content of 44.12%, 137 tRNA genes and 46 rRNA genes [52]. In contrast, the whole genome of the novel strain *Vibrio* sp. J383 has a total of 16 (5S), 15 (16S), and 15 (23S) rRNAs, 138 tRNAs, and 5 ncRNAs (Table 4). These results suggest that although *V. splendidus* and *Vibrio* sp. J383 share a common ancestor, they are different strains with distinct genomic characteristics.

Some specific genes associated with virulence and antibiotic resistance were detected in the PATRIC comprehensive genome analysis. The tetracycline resistance subsystem was found in *Vibrio* sp. J383, which makes this strain resistant to antibiotics and toxic compounds. Hydroxyacylglutathione hydrolase was also found in *Vibrio* sp. J383, which is a virulence-related gene and contributes to the stress response in bacteria.

Cold shock proteins of the CSP family were found in chromosome 2 of *Vibrio* sp. J383 (Table S2). Cold shock proteins help cells adapt by reducing some of the negative effects of temperature changes [53]. They play a crucial role in the cold shock response, and recent data suggest that CSPs may have a greater role in bacterial stress tolerance [54–56]. Following the initial cold shock response, the production of CSPs declines while the production of other proteins increases. This helps the cells to grow at a low temperature, but at a slower rate [57]. This finding can explain why *Vibrio* sp. J383 has fast growth at 15 °C and slightly slower growth at 4 °C (Table 1).

Flagellum was detected in chromosome 1 of *Vibrio* sp. J383 (Table S2), which plays a key role in bacteria motility, and can contribute to biofilm formation, protein export and adhesion [58]. Chemotaxis present in chromosome 1 of *Vibrio* sp. J383 plays several roles, including biofilm formation, auto aggregation and swarming, as well as in bacterial interactions with their hosts [59]. Toxin–antitoxin systems are common in bacterial genomes and found in chromosome 2 of *Vibrio* sp. J383 (Table S2). They are normally made of two elements: a toxin that inhibits a vital cellular process and an antitoxin that hinders its cognate toxin [60].

A total of 24 genomic islands were detected in *Vibrio* sp. J383. Genomic Islands have also been identified in the species *V. anguillarum*. For example, *V. anguillarum* J360 has 21 GIs [15]. Genes encoding for integrase and transposase were found in the mentioned *Vibrio* strains. Glutaredoxin was detected in chromosome 2 of *Vibrio* sp. J383, and performs a critical role in the protection against oxidative stress in bacteria [61]. VirK is a virulence factor present in several bacterial pathogens that has been shown to contribute to *Salmonella enterica* serovar Typhimurium and *Escherichia coli* virulence [62–64]. It may contribute to *Vibrio* sp.’s pathogenicity as well. Also, Zot was detected in the genomes of *V. parahaemolyticus* [65], indicating a correlation between this gene and the cytotoxicity of bacteria [65,66]. In *V. cholerae*, Zot is an important toxin after the classical cholera toxin (CT), and it is encoded by the CTX prophage [67]. It has been shown that Zot has enterotoxic activity and it is hypothesized that it plays a role in the classic diarrhea symptom of *V. cholerae* infections [68,69]. The presence of Zot in the genome of *Vibrio* sp. J383 perhaps contributes to its virulence in fish hosts.

The T6SS is a contractile nanomachine that plays a role in interbacterial competition and bacterial pathogenesis by secreting toxic effector proteins into adjacent cells [70–75]. The *Vibrio* sp. J383 genome includes two T6SSs on genomic islands 12 and 21 (Table 5, Figure 7, and Supplementary File S4). T6SS apparatuses are composed of 13 core components that form two parts, the membrane complex and phage-like tail [76,77]. Three membrane-associated proteins comprise the membrane complex, TssJ, TssL, and TssM [75,76,78,79]. Consistent with this, the *Vibrio* sp. J383 homologs are predicted to be lipidated or to contain transmembrane domains. The T6SS tail is evolutionarily related to the contractile tail of the T4 bacteriophage and is composed of several subassemblies. The baseplate is composed of *tssE*, *tssF*, *tssG*, and *tssK* [80,81], and the *Vibrio* sp. J383 homologs share 60–80% identity with other *Vibrio* T6SS counterparts. *tssB*, *tssC*, and *tssA* comprise the sheath and cap of the T6SS and are encoded in both loci [82–84]. Of note, *tssB* and *tssC* share greater than 95% identity with other *Vibrio* T6SSs. Hcp and VgrG play a role in substrate recognition and

are co-secreted with associated toxins, and both are encoded in the T6SS loci in *Vibrio* sp. J383 [76,78,85].

The genes that encode these T6SS apparatus subunits share high levels of homology between genomic islands 12 and 21. Based on homology with well-characterized T6SSs, both apparatuses encoded by *Vibrio* sp. J383 belong to the T6SSⁱ family. It is impossible to identify T6SS-exported toxins based on sequence alone; however, some of the hypothetical genes in these two loci encode hallmarks that suggest that they may be effector proteins. The presence of toxic effector genes in close proximity to T6SS apparatus genes does not preclude other effectors encoded in distant genomic loci, and further research can identify these toxins in the future.

Gene duplications are essential prerequisites for gene innovation, which may assist in adaptation to changing environmental conditions [86]. In chromosome 1 of *Vibrio* sp. J383, *tssC* is duplicated (Figure 7). T6SSs have been strongly linked to a variety of biological processes, including biofilm formation, bacterial survival in the environment, virulence, and host adaptation; therefore, the duplication of *tssC* in *Vibrio* sp. J383 may be an important step toward increasing the fitness of this strain in the environment, amongst the microbiota, or as a pathogen [87–89].

In summary, *Vibrio* sp. J383 has several virulence factors and genes that are associated with pathogens.

Vibrio sp. J383 has one large plasmid, and an analysis based on PATRIC annotation found one subsystem, the MazEF toxin–antitoxin (program cell death) system (Table S2). Toxin–antitoxin (TA) systems, initially discovered in plasmids, were recognized as extra-chromosomal genes responsible for post-segregationally killing, which protects plasmid integrity [90]. Toxin–antitoxin (TA) systems have been reported in many bacterial genomes and mediate program cell death (PCD), and are therefore attractive targets for new antimicrobial drugs since they are recognized to “kill from within” [91,92]. The antitoxins neutralize the toxin using different mechanisms and play vital roles, including the maintenance of genomic stability, and assist in biofilm formation in some bacteria [90]. The presence of the TA system in the plasmid of *Vibrio* sp. J383 indicates that it may play may the same role and enable *Vibrio* sp. J383 to survive in different temperatures and maintain its virulence factors.

5. Conclusions

The biochemical profile showed that *Vibrio* sp. J383 is similar to *V. vulnificus*, with 64.8% identity. However, phylogenetic and comparative analyses showed that *Vibrio* sp. J383 is closely related to *V. splendidus*, with 93% identity. The isolation of *Vibrio* sp. J383 from blood samples confirmed Koch’s postulates. Mortality was approximately 20% in the vaccinated fish infected with a 10^8 CFU/dose, but no mortality was observed in fish infected with a low dose (10^6 CFU/dose). *Vibrio* sp. J383 was detected for 10 wpi in the blood and at up to 14 wpi in the internal organs (spleen and kidney). The pathogenicity of this new strain is supported by Koch’s postulates and the presence of pathogenic genomic islands (GIs 12 and 21) containing virulence factors such as type VI secretion system (T6SS) genes and multidrug-resistance transporter/family protein. *Vibrio* sp. J383 displays unique characteristics, and has notable differences, compared to other *Vibrio* strains. The results of this study revealed that *Vibrio* sp. J383 is potentially a new species that can trigger clinical signs of ulcer disease and cause chronic infections in vaccinated farmed Atlantic salmon. The impact of the co-infection of *Vibrio* sp. J383 with other etiological agents, like *Moritella viscosa*, on Atlantic salmon remains to be investigated.

Supplementary Materials: The following supporting information can be downloaded at: <https://www.mdpi.com/article/10.3390/microorganisms11071736/s1>, Figure S1: Phenotypic characteristics of *Vibrio* sp. J383, Figure S2: Acute mortality of Atlantic salmon infected with different bacterial strains isolated from fish exhibiting ‘winter ulcer’-like clinical signs, Figure S3: (A) Average nucleotide identity in *Vibrio* sp. J383. chromosome 1, and (B) average nucleotide identity in *Vibrio* sp. J383. chromosome 2, Table S1: Enzymatic profile of *Vibrio* sp. J383 using commercial biochemical

test kits (API system), Table S2. Genes associated with subsystems in chromosomes and plasmid, Supplementary File S1: Genomic Islands (GIs) of *Vibrio* sp. J383-chromosome 1, Supplementary File S2: Genomic Islands (GIs) of *Vibrio* sp. J383-chromosome 2, Supplementary File S3: Genomic Islands (GIs) of *Vibrio* sp. J383-plasmid, Supplementary File S4: T6SS genes in *Vibrio* sp. J383, Supplementary File S5: Comparison of GI21 to GI12.

Author Contributions: Conceptualization, M.G., A.K.G. and J.S.; methodology, M.G. and J.S.; software, M.G., J.S., A.E. and I.V.; formal analysis, M.G., I.V., A.E. and J.S.; investigation, M.G. and J.S.; resources, J.S. and A.K.G.; data curation, M.G., A.E., J.S. and I.V.; writing—original draft preparation, M.G. and J.S.; writing—review and editing, M.G., I.V., A.E., A.K.G. and J.S.; visualization: M.G.; supervision, J.S.; funding acquisition, J.S. and A.K.G. All authors have read and agreed to the published version of the manuscript.

Funding: This work was funded through grants from the Canada First Excellence Research Fund—Ocean Frontier Institute (sub-module J3), an NSERC-Discovery grant (RGPIN-2018-05942), funding from the Canadian Center for Fisheries and Innovation (CCFI; grant number A-2020-02), Innovate NL (contract number 5404-1209-106) and by Cooke Aquaculture Inc.

Data Availability Statement: Not applicable.

Acknowledgments: The authors thank Santander’s and Gamperl’s lab members, and the Department of Ocean Sciences and the Cold Ocean Deep Sea Research Facility staff for providing technical assistance (fish holding and transferring) in this research.

Conflicts of Interest: The authors declare no conflict of interest.

References

1. Lunder, T. Vintersir [Winter ulcer]. In *Fisk. [Fish Health]*; Poppe, T.T., Ed.; John Grieg Forlag: Bergen, Norway, 1990; pp. 304–305.
2. Benediktsdóttir, E.; Verdonck, L.; Spröer, C.; Helgason, S.; Swings, J. Characterization of *Vibrio viscosus* and *Vibrio wodanis* isolated at different geographical locations: A proposal for reclassification of *Vibrio viscosus* as *Moritella viscosa* comb. nov. *Int. J. Syst. Evol. Microbiol.* **2000**, *50*, 479–488. [[CrossRef](#)] [[PubMed](#)]
3. Løvoll, M.; Wiik-Nielsen, C.; Tunsjø, H.S.; Colquhoun, D.; Lunder, T.; Sørum, H.; Grove, S. Atlantic salmon bath challenged with *Moritella viscosa*—pathogen invasion and host response. *Fish Shellfish Immunol.* **2009**, *26*, 877–884. [[CrossRef](#)] [[PubMed](#)]
4. Benediktsdóttir, E.; Helgason, S.; Sigurjónsdóttir, H. *Vibrio* spp. isolated from salmonids with shallow skin lesions and reared at low temperature. *J. Fish Dis.* **1998**, *21*, 19–28. [[CrossRef](#)]
5. Olsen, A.B.; Nilsen, H.; Sandlund, N.; Mikkelsen, H.; Sørum, H.; Colquhoun, D. *Tenacibaculum* sp. associated with winter ulcers in sea-reared Atlantic salmon *Salmo salar*. *Dis. Aquat. Org.* **2011**, *94*, 189–199. [[CrossRef](#)] [[PubMed](#)]
6. Hjerde, E.; Karlsen, C.; Sørum, H.; Parkhill, J.; Willlassen, N.P.; Thomson, N.R. Co-cultivation and transcriptome sequencing of two co-existing fish pathogens *Moritella viscosa* and *Aliivibrio wodanis*. *BMC Genom.* **2015**, *16*, 447. [[CrossRef](#)]
7. Karlsen, C.; Vanberg, C.; Mikkelsen, H.; Sørum, H. Co-infection of Atlantic salmon (*Salmo salar*), by *Moritella viscosa* and *Aliivibrio wodanis*, development of disease and host colonization. *Vet. Microbiol.* **2014**, *171*, 112–121. [[CrossRef](#)]
8. Whitman, K.; Backman, S.; Benediktsdóttir, E.; Coles, M.; Johnson, G.R. Isolation and characterization of a new *Vibrio* spp. (*Vibrio wodanis*) associated with ‘winter ulcer disease’ in sea water raised Atlantic salmon (*Salmo salar* L.) in New Brunswick. In *Aquaculture Canada 2000*; Aquaculture Association of Canada: Moncton, NB, Canada, 2001; Volume 4, pp. 115–117.
9. Lunder, T.; Evensen, Ø.; Holstad, G.; Håstein, T. ‘Winter ulcer’ in the Atlantic salmon *Salmo salar*. Pathological and bacteriological investigations and transmission experiments. *Dis. Aquat. Org.* **1995**, *23*, 39–49. [[CrossRef](#)]
10. Furevik, A.; Tunheim, S.H.; Heen, V.; Klevan, A.; Knutsen, L.E.; Tandberg, J.I.; Tingbo, M.G. New vaccination strategies are required for effective control of winter ulcer disease caused by emerging variant strains of *Moritella viscosa* in Atlantic salmon. *Fish Shellfish Immunol.* **2023**, *137*, 108784. [[CrossRef](#)]
11. Karlsen, C.; Thorarinsson, R.; Wallace, C.; Saloniemi, K.; Midtlyng, P.J. Atlantic salmon winter-ulcer disease: Combining mortality and skin ulcer development as clinical efficacy criteria against *Moritella viscosa* infection. *Aquaculture* **2017**, *473*, 538–544. [[CrossRef](#)]
12. Tunsjø, H.S.; Paulsen, S.M.; Mikkelsen, H.; L’Abée-Lund, T.M.; Skjerve, E.; Sørum, H. Adaptive response to environmental changes in the fish pathogen *Moritella viscosa*. *Res. Microbiol.* **2007**, *158*, 244–250. [[CrossRef](#)]
13. MacKinnon, B.; Jones, P.; Hawkins, L.; Dohoo, I.; Stryhn, H.; Vanderstichel, R.; St-Hilaire, S. The epidemiology of skin ulcers in saltwater reared Atlantic salmon (*Salmo salar*) in Atlantic Canada. *Aquaculture* **2019**, *501*, 230–238. [[CrossRef](#)]
14. MacKinnon, B.; Groman, D.; Fast, M.D.; Manning, A.J.; Jones, P.; St-Hilaire, S. Atlantic salmon challenged with extracellular products from *Moritella viscosa*. *Dis. Aquat. Org.* **2019**, *133*, 119–125. [[CrossRef](#)] [[PubMed](#)]
15. Vasquez, I.; Cao, T.; Chakraborty, S.; Gnanagobal, H.; O’Brien, N.; Monk, J.; Boyce, D.; Westcott, J.D.; Santander, J. Comparative Genomics Analysis of *Vibrio anguillarum* Isolated from Lumpfish (*Cyclopterus lumpus*) in Newfoundland Reveal Novel Chromosomal Organizations. *Microorganisms* **2020**, *8*, 1666. [[CrossRef](#)] [[PubMed](#)]

16. Leboffe, M.J.; Pierce, B.E. *Microbiology: Laboratory Theory and Application*; Morton Publishing Company: Englewood, CO, USA, 2015.
17. Soto-Dávila, M.; Hossain, A.; Chakraborty, S.; Rise, M.L.; Santander, J. *Aeromonas salmonicida* subsp. *salmonicida* early infection and immune response of Atlantic cod (*Gadus morhua* L.) primary macrophages. *Front. Immunol.* **2019**, *10*, 1237. [[CrossRef](#)]
18. Connors, E.; Soto-Dávila, M.; Hossain, A.; Vasquez, I.; Gnanagobal, H.; Santander, J. Identification and validation of reliable *Aeromonas salmonicida* subspecies *salmonicida* reference genes for differential gene expression analyses. *Infect. Genet. Evol.* **2019**, *73*, 314–321. [[CrossRef](#)]
19. Myhr, E.; Larsen, J.L.; Lillehaug, A.; Gudding, R.; Heum, M.; Håstein, T. Characterization of *Vibrio anguillarum* and closely related species isolated from farmed fish in Norway. *Appl. Environ. Microbiol.* **1991**, *57*, 2750–2757. [[CrossRef](#)]
20. Wood, E. *Molecular Cloning: A Laboratory Manual*; Maniatis, T., Fritsch, E.F., Sambrook, J., Eds.; Cold Spring Harbor Laboratory: New York, NY, USA, 1982; p. 545. ISBN 0-87969-136-0.
21. Hitchcock, P.J.; Brown, T. Morphological heterogeneity among *Salmonella* lipopolysaccharide chemotypes in silver-stained polyacrylamide gels. *J. Bacteriol.* **1983**, *154*, 269–277. [[CrossRef](#)]
22. Santander, J.; Martin, T.; Loh, A.; Pohlenz, C.; Gatlin, D.M., III; Curtiss, R., III. Mechanisms of intrinsic resistance to antimicrobial peptides of *Edwardsiella ictaluri* and its influence on fish gut inflammation and virulence. *Microbiology* **2013**, *159*, 1471. [[CrossRef](#)]
23. Ramasam, P.; Sujatha Ran, J.; Gunasekaran, D.R. Assessment of antibiotic sensitivity and pathogenicity of *Vibrio* spp. and *Aeromonas* spp. from aquaculture environment. *MOJ Eco. Environ. Sci.* **2018**, *3*, 128–136.
24. Louden, B.C.; Haarmann, D.; Lynne, A.M. Use of blue agar CAS assay for siderophore detection. *J. Microbiol. Biol. Educ.* **2011**, *12*, 51–53. [[CrossRef](#)]
25. Vasquez, I.; Cao, T.; Hossain, A.; Valderrama, K.; Gnanagobal, H.; Dang, M.; Leeuwis, R.H.; Ness, M.; Campbell, B.; Gendron, R. *Aeromonas salmonicida* infection kinetics and protective immune response to vaccination in sablefish (*Anoplopoma fimbria*). *Fish Shellfish Immunol.* **2020**, *104*, 557–566. [[CrossRef](#)]
26. Umasuthan, N.; Valderrama, K.; Vasquez, I.; Segovia, C.; Hossain, A.; Cao, T.; Gnanagobal, H.; Monk, J.; Boyce, D.; Santander, J. A novel marine pathogen isolated from wild cunners (*Tautogolabrus adspersus*): Comparative genomics and transcriptome profiling of *Pseudomonas* sp. strain J380. *Microorganisms* **2021**, *9*, 812. [[CrossRef](#)] [[PubMed](#)]
27. Koch, R. Ueber den augenblicklichen Stand der bakteriologischen Choleradiagnose. *Z. Hyg. Infekt.* **1893**, *14*, 319–338. [[CrossRef](#)]
28. Chakraborty, S.; Cao, T.; Hossain, A.; Gnanagobal, H.; Vasquez, I.; Boyce, D.; Santander, J. Vibrogen-2 vaccine trial in lumpfish (*Cyclopterus lumpus*) against *Vibrio anguillarum*. *J. Fish Dis.* **2019**, *42*, 1057–1064. [[CrossRef](#)]
29. Sambrook, J.; Russell, D. *Molecular Cloning: A Laboratory Manual*, 3rd ed.; Cold Spring Harbor Lab. Press: Plainview, NY, USA, 2001.
30. Aziz, R.K.; Bartels, D.; Best, A.A.; DeJongh, M.; Disz, T.; Edwards, R.A.; Formsma, K.; Gerdes, S.; Glass, E.M.; Kubal, M. The RAST Server: Rapid annotations using subsystems technology. *BMC Genom.* **2008**, *9*, 75. [[CrossRef](#)] [[PubMed](#)]
31. Overbeek, R.; Olson, R.; Pusch, G.D.; Olsen, G.J.; Davis, J.J.; Disz, T.; Edwards, R.A.; Gerdes, S.; Parrello, B.; Shukla, M. The SEED and the Rapid Annotation of microbial genomes using Subsystems Technology (RAST). *Nucleic Acids Res.* **2014**, *42*, D206–D214. [[CrossRef](#)] [[PubMed](#)]
32. Davis, J.J.; Wattam, A.R.; Aziz, R.K.; Brettin, T.; Butler, R.; Butler, R.M.; Chlenski, P.; Conrad, N.; Dickerman, A.; Dietrich, E.M. The PATRIC Bioinformatics Resource Center: Expanding data and analysis capabilities. *Nucleic Acids Res.* **2020**, *48*, D606–D612. [[CrossRef](#)]
33. Tamura, K.; Stecher, G.; Kumar, S. MEGA11: Molecular evolutionary genetics analysis version 11. *Mol. Biol. Evol.* **2021**, *38*, 3022–3027. [[CrossRef](#)]
34. Saitou, N.; Nei, M. The neighbor-joining method: A new method for reconstructing phylogenetic trees. *Mol. Biol. Evol.* **1987**, *4*, 406–425.
35. Jukes, T.H.; Cantor, C.R. Evolution of protein molecules. *Mamm. Protein Metab.* **1969**, *3*, 21–132.
36. Teru, Y.; Hikima, J.-I.; Kono, T.; Sakai, M.; Takano, T.; Hawke, J.P.; Takeyama, H.; Aoki, T. Whole-genome sequence of *Photobacterium damsela* subsp. *piscicida* strain 91-197, isolated from hybrid striped bass (*Morone* sp.) in the United States. *Genome Announc.* **2017**, *5*, e00600–e00617. [[CrossRef](#)]
37. Bertelli, C.; Laird, M.R.; Williams, K.P.; Simon Fraser University Research Computing Group; Lau, B.Y.; Hoad, G.; Winsor, G.L.; Brinkman, F.S. IslandViewer 4: Expanded prediction of genomic islands for larger-scale datasets. *Nucleic Acids Res.* **2017**, *45*, W30–W35. [[CrossRef](#)] [[PubMed](#)]
38. Li, J.; Yao, Y.; Xu, H.H.; Hao, L.; Deng, Z.; Rajakumar, K.; Ou, H.Y. SecReT6: A web-based resource for type VI secretion systems found in bacteria. *Environ. Microbiol.* **2015**, *17*, 2196–2202. [[CrossRef](#)] [[PubMed](#)]
39. Zhang, J.; Guan, J.; Wang, M.; Li, G.; Djordjevic, M.; Tai, C.; Wang, H.; Deng, Z.; Chen, Z.; Ou, H.-Y. SecReT6 update: A comprehensive resource of bacterial Type VI Secretion Systems. *Sci. China Life Sci.* **2023**, *66*, 626–634. [[CrossRef](#)] [[PubMed](#)]
40. Machimbirike, V.I.; Vasquez, I.; Cao, T.; Chukwu-Osazuwa, J.; Onireti, O.; Segovia, C.; Khunrae, P.; Rattanarojpong, T.; Booman, M.; Jones, S. Comparative Genomic Analysis of Virulent *Vibrio* (*Listonella*) *anguillarum* Serotypes Revealed Genetic Diversity and Genomic Signatures in the O-Antigen Biosynthesis Gene Cluster. *Microorganisms* **2023**, *11*, 792. [[CrossRef](#)]
41. Jumper, J.; Evans, R.; Pritzel, A.; Green, T.; Figurnov, M.; Ronneberger, O.; Tunyasuvunakool, K.; Bates, R.; Žídek, A.; Potapenko, A. Highly accurate protein structure prediction with AlphaFold. *Nature* **2021**, *596*, 583–589. [[CrossRef](#)]

42. Guillemette, R.; Ushijima, B.; Jalan, M.; Häse, C.C.; Azam, F. Insight into the resilience and susceptibility of marine bacteria to T6SS attack by *Vibrio cholerae* and *Vibrio coralliilyticus*. *PLoS ONE* **2020**, *15*, e0227864. [[CrossRef](#)]
43. Darling, A.C.; Mau, B.; Blattner, F.R.; Perna, N.T. Mauve: Multiple alignment of conserved genomic sequence with rearrangements. *Genome Res.* **2004**, *14*, 1394–1403. [[CrossRef](#)]
44. Miethke, M.; Marahiel, M.A. Siderophore-based iron acquisition and pathogen control. *Microbiol. Mol. Biol. Rev.* **2007**, *71*, 413–451. [[CrossRef](#)]
45. Alsina, M.; Blanch, A.R. A set of keys for biochemical identification of environmental *Vibrio* species. *J. Appl. Bacteriol.* **1994**, *76*, 79–85. [[CrossRef](#)]
46. Sadok, K.; Mejdi, S.; Nourhen, S.; Amina, B. Phenotypic characterization and RAPD fingerprinting of *Vibrio parahaemolyticus* and *Vibrio alginolyticus* isolated during Tunisian fish farm outbreaks. *Folia Microbiol.* **2013**, *58*, 17–26. [[CrossRef](#)] [[PubMed](#)]
47. Johnson, C.N. Fitness factors in vibrios: A mini-review. *Microb. Ecol.* **2013**, *65*, 826–851. [[CrossRef](#)] [[PubMed](#)]
48. Hirono, I.; Masuda, T.; Aoki, T. Cloning and detection of the hemolysin gene of *Vibrio anguillarum*. *Microb. Pathog.* **1996**, *21*, 173–182. [[CrossRef](#)]
49. Rock, J.L.; Nelson, D.R. Identification and characterization of a hemolysin gene cluster in *Vibrio anguillarum*. *Infect. Immun.* **2006**, *74*, 2777–2786. [[CrossRef](#)] [[PubMed](#)]
50. Lunder, T.; Sørum, H.; Holstad, G.; Steigerwalt, A.G.; Mowinkel, P.; Brenner, D.J. Phenotypic and genotypic characterization of *Vibrio viscosus* sp. nov. and *Vibrio wodanis* sp. nov. isolated from Atlantic salmon (*Salmo salar*) with ‘winter ulcer’. *Int. J. Syst. Evol. Microbiol.* **2000**, *50*, 427–450. [[CrossRef](#)] [[PubMed](#)]
51. Frans, I.; Michiels, C.W.; Bossier, P.; Willems, K.; Lievens, B.; Rediers, H. *Vibrio anguillarum* as a fish pathogen: Virulence factors, diagnosis and prevention. *J. Fish Dis.* **2011**, *34*, 643–661. [[CrossRef](#)]
52. Park, J.W.; Lee, S.-E.; Shin, W.-S.; Kim, K.J.; Kim, Y.U. Draft genome sequences of *Vibrio splendidus* KCTC 11899BP, which produces hyaluronate lyase in the presence of hyaluronic acid. *Korean J. Microbiol.* **2018**, *54*, 302–304.
53. Phadtare, S. Recent developments in bacterial cold-shock response. *Curr. Issues Mol. Biol.* **2004**, *6*, 125–136.
54. Schmid, B.; Klumpp, J.; Raimann, E.; Loessner, M.J.; Stephan, R.; Tasara, T. Role of cold shock proteins in growth of *Listeria monocytogenes* under cold and osmotic stress conditions. *Appl. Environ. Microbiol.* **2009**, *75*, 1621–1627. [[CrossRef](#)]
55. Wang, Z.; Wang, S.; Wu, Q. Cold shock protein A plays an important role in the stress adaptation and virulence of *Brucella melitensis*. *FEMS Microbiol. Lett.* **2014**, *354*, 27–36. [[CrossRef](#)]
56. Derman, Y.; Söderholm, H.; Lindström, M.; Korkeala, H. Role of csp genes in NaCl, pH, and ethanol stress response and motility in *Clostridium botulinum* ATCC 3502. *Food Microbiol.* **2015**, *46*, 463–470. [[CrossRef](#)] [[PubMed](#)]
57. Ermolenko, D.; Makhatadze, G. Bacterial cold-shock proteins. *Cell. Mol. Life Sci. CMS* **2002**, *59*, 1902–1913. [[CrossRef](#)] [[PubMed](#)]
58. Haiko, J.; Westerlund-Wikström, B. The role of the bacterial flagellum in adhesion and virulence. *Biology* **2013**, *2*, 1242–1267. [[CrossRef](#)]
59. Colin, R.; Ni, B.; Laganenka, L.; Sourjik, V. Multiple functions of flagellar motility and chemotaxis in bacterial physiology. *FEMS Microbiol. Rev.* **2021**, *45*, fuab038. [[CrossRef](#)]
60. Jurénas, D.; Fraikin, N.; Goormaghtigh, F.; Van Melderen, L. Biology and evolution of bacterial toxin–antitoxin systems. *Nat. Rev. Microbiol.* **2022**, *20*, 335–350. [[CrossRef](#)] [[PubMed](#)]
61. Laporte, D.; Olate, E.; Salinas, P.; Salazar, M.; Jordana, X.; Holuigue, L. Glutaredoxin GRXS13 plays a key role in protection against photooxidative stress in *Arabidopsis*. *J. Exp. Bot.* **2012**, *63*, 503–515. [[CrossRef](#)]
62. Detweiler, C.S.; Monack, D.M.; Brodsky, I.E.; Mathew, H.; Falkow, S. virK, somA and rcsC are important for systemic *Salmonella enterica* serovar *Typhimurium* infection and cationic peptide resistance. *Mol. Microbiol.* **2003**, *48*, 385–400. [[CrossRef](#)]
63. Song, J.; Hou, H.-M.; Wu, H.-Y.; Li, K.-X.; Wang, Y.; Zhou, Q.-Q.; Zhang, G.-L. Transcriptomic analysis of *Vibrio parahaemolyticus* reveals different virulence gene expression in response to benzyl isothiocyanate. *Molecules* **2019**, *24*, 761. [[CrossRef](#)]
64. Tapia-Pastrana, G.; Chavez-Dueñas, L.; Lanz-Mendoza, H.; Teter, K.; Navarro-Garcia, F. VirK is a periplasmic protein required for efficient secretion of plasmid-encoded toxin from enteroaggregative *Escherichia coli*. *Infect. Immun.* **2012**, *80*, 2276–2285. [[CrossRef](#)]
65. Pérez-Reytor, D.; Pavón, A.; Lopez-Joven, C.; Ramírez-Araya, S.; Peña-Varas, C.; Plaza, N.; Alegria-Arcos, M.; Corsini, G.; Jaña, V.; Pavez, L. Analysis of the Zonula occludens Toxin Found in the Genome of the Chilean Non-toxigenic *Vibrio parahaemolyticus* Strain PMC53. *7. Front. Cell. Infect. Microbiol.* **2020**, *10*, 482. [[CrossRef](#)]
66. Castillo, D.; Pérez-Reytor, D.; Plaza, N.; Ramírez-Araya, S.; Blondel, C.J.; Corsini, G.; Bastías, R.; Loyola, D.E.; Jaña, V.; Pavez, L. Exploring the genomic traits of non-toxigenic *Vibrio parahaemolyticus* strains isolated in southern Chile. *Front. Microbiol.* **2018**, *9*, 161. [[CrossRef](#)]
67. Schmidt, E.; Kelly, S.; Van Der Walle, C. Tight junction modulation and biochemical characterisation of the zonula occludens toxin C-and N-termini. *FEBS Lett.* **2007**, *581*, 2974–2980. [[CrossRef](#)]
68. Fasano, A.; Baudry, B.; Pumplin, D.W.; Wasserman, S.S.; Tall, B.D.; Ketley, J.M.; Kaper, J. *Vibrio cholerae* produces a second enterotoxin, which affects intestinal tight junctions. *Proc. Natl. Acad. Sci. USA* **1991**, *88*, 5242–5246. [[CrossRef](#)]
69. Suzuki, T. Regulation of intestinal epithelial permeability by tight junctions. *Cell. Mol. Life Sci.* **2013**, *70*, 631–659. [[CrossRef](#)] [[PubMed](#)]
70. Russell, A.B.; Hood, R.D.; Bui, N.K.; LeRoux, M.; Vollmer, W.; Mougous, J.D. Type VI secretion delivers bacteriolytic effectors to target cells. *Nature* **2011**, *475*, 343–347. [[CrossRef](#)] [[PubMed](#)]

71. Russell, A.B.; Peterson, S.B.; Mougous, J.D. Type VI secretion system effectors: Poisons with a purpose. *Nat. Rev. Microbiol.* **2014**, *12*, 137–148. [[CrossRef](#)]
72. Crisan, C.V.; Hammer, B.K. The *Vibrio cholerae* type VI secretion system: Toxins, regulators and consequences. *Environ. Microbiol.* **2020**, *22*, 4112–4122. [[CrossRef](#)]
73. Zong, B.; Zhang, Y.; Wang, X.; Liu, M.; Zhang, T.; Zhu, Y.; Zheng, Y.; Hu, L.; Li, P.; Chen, H. Characterization of multiple type-VI secretion system (T6SS) VgrG proteins in the pathogenicity and antibacterial activity of porcine extra-intestinal pathogenic *Escherichia coli*. *Virulence* **2019**, *10*, 118–132. [[CrossRef](#)]
74. Hachani, A.; Lossi, N.S.; Hamilton, A.; Jones, C.; Bleves, S.; Albesa-Jové, D.; Filloux, A. Type VI secretion system in *Pseudomonas aeruginosa*: Secretion and multimerization of VgrG proteins. *J. Biol. Chem.* **2011**, *286*, 12317–12327. [[CrossRef](#)]
75. Bingle, L.E.; Bailey, C.M.; Pallen, M.J. Type VI secretion: A beginner’s guide. *Curr. Opin. Microbiol.* **2008**, *11*, 3–8. [[CrossRef](#)] [[PubMed](#)]
76. Boyer, F.; Fichant, G.; Berthod, J.; Vandenbrouck, Y.; Attree, I. Dissecting the bacterial type VI secretion system by a genome wide in silico analysis: What can be learned from available microbial genomic resources? *BMC Genom.* **2009**, *10*, 104. [[CrossRef](#)] [[PubMed](#)]
77. Cherrak, Y.; Flauggnatti, N.; Durand, E.; Journet, L.; Cascales, E. Structure and activity of the type VI secretion system. *Microbiol. Spectr.* **2019**. [[CrossRef](#)] [[PubMed](#)]
78. Cascales, E. The type VI secretion toolkit. *EMBO Rep.* **2008**, *9*, 735–741. [[CrossRef](#)]
79. Aschtgen, M.S.; Gavioli, M.; Dessen, A.; Lloubès, R.; Cascales, E. The SciZ protein anchors the enteroaggregative *Escherichia coli* Type VI secretion system to the cell wall. *Mol. Microbiol.* **2010**, *75*, 886–899. [[CrossRef](#)] [[PubMed](#)]
80. Cherrak, Y.; Rapisarda, C.; Pelliarin, R.; Bouvier, G.; Bardiaux, B.; Allain, F.; Malosse, C.; Rey, M.; Chamot-Rooke, J.; Cascales, E. Biogenesis and structure of a type VI secretion baseplate. *Nat. Microbiol.* **2018**, *3*, 1404–1416. [[CrossRef](#)]
81. Taylor, N.M.; Prokhorov, N.S.; Guerrero-Ferreira, R.C.; Shneider, M.M.; Browning, C.; Goldie, K.N.; Stahlberg, H.; Leiman, P.G. Structure of the T4 baseplate and its function in triggering sheath contraction. *Nature* **2016**, *533*, 346–352. [[CrossRef](#)] [[PubMed](#)]
82. Bönemann, G.; Pietrosiuk, A.; Mogk, A. Tubules and donuts: A type VI secretion story. *Mol. Microbiol.* **2010**, *76*, 815–821. [[CrossRef](#)]
83. Basler, Á.; Pilhofer, Á.; Henderson, G.; Jensen, G.; Mekalanos, J. Type VI secretion requires a dynamic contractile phage tail-like structure. *Nature* **2012**, *483*, 182–186. [[CrossRef](#)]
84. Zoued, A.; Durand, E.; Santin, Y.G.; Journet, L.; Roussel, A.; Cambillau, C.; Cascales, E. TssA: The cap protein of the type VI secretion system tail. *Bioessays* **2017**, *39*, 1600262. [[CrossRef](#)]
85. Alteri, C.J.; Mobley, H.L. The versatile type VI secretion system. *Microbiol. Spectr.* **2016**, *4*. [[CrossRef](#)]
86. Gevers, D.; Vandepoele, K.; Simillion, C.; Van de Peer, Y. Gene duplication and biased functional retention of paralogs in bacterial genomes. *Trends Microbiol.* **2004**, *12*, 148–154. [[CrossRef](#)] [[PubMed](#)]
87. Chen, L.; Zou, Y.; Kronfl, A.A.; Wu, Y. Type VI secretion system of *Pseudomonas aeruginosa* is associated with biofilm formation but not environmental adaptation. *Microbiologyopen* **2020**, *9*, e991. [[CrossRef](#)] [[PubMed](#)]
88. Yu, K.-W.; Xue, P.; Fu, Y.; Yang, L. T6SS mediated stress responses for bacterial environmental survival and host adaptation. *Int. J. Mol. Sci.* **2021**, *22*, 478. [[CrossRef](#)]
89. Masum, M.M.I.; Yang, Y.; Li, B.; Olaitan, O.S.; Chen, J.; Zhang, Y.; Fang, Y.; Qiu, W.; Wang, Y.; Sun, G. Role of the genes of type VI secretion system in virulence of rice bacterial brown stripe pathogen *Acidovorax avenae* subsp. *avenae* strain RS-2. *Int. J. Mol. Sci.* **2017**, *18*, 2024. [[CrossRef](#)] [[PubMed](#)]
90. Ramisetty, B.C.M.; Natarajan, B.; Santhosh, R.S. mazEF-mediated programmed cell death in bacteria: “what is this?”. *Crit. Rev. Microbiol.* **2015**, *41*, 89–100. [[CrossRef](#)]
91. Amitai, S.; Kolodkin-Gal, I.; Hananya-Meltabashi, M.; Sacher, A.; Engelberg-Kulka, H. *Escherichia coli* MazF leads to the simultaneous selective synthesis of both “death proteins” and “survival proteins”. *PLoS Genet.* **2009**, *5*, e1000390. [[CrossRef](#)] [[PubMed](#)]
92. Engelberg-Kulka, H.; Yelin, I.; Kolodkin-Gal, I. Activation of a built-in bacterial programmed cell death system as a novel mechanism of action of some antibiotics. *Commun. Integr. Biol.* **2009**, *2*, 211–212. [[CrossRef](#)]

Disclaimer/Publisher’s Note: The statements, opinions and data contained in all publications are solely those of the individual author(s) and contributor(s) and not of MDPI and/or the editor(s). MDPI and/or the editor(s) disclaim responsibility for any injury to people or property resulting from any ideas, methods, instructions or products referred to in the content.